ISBN: 978-3-95450-262-2 ISSN: 2673-5350 doi: 10.18429/JACoW-IBIC2025-WEPMO29

APPLICATION OF PHASE DETECTORS AT THE TAIWAN PHOTON SOURCE

C. H. Huang*, K. T. Hsu, S.-H. Lee, P. C. Chiu, K. H. Hu, C. Y. Wu
National Synchrotron Radiation Research Center (NSRRC), Hsinchu, Taiwan

Abstract

A phase detection system has been implemented at the Taiwan Photon Source, employing beam position monitor electronics integrated with a digital in-phase/quadrature (I/Q) demodulation scheme. This system enables high-resolution analysis of beam phase stability, radio-frequency (RF) cavity field phase, and synchronization integrity of the RF clock distribution. It also facilitates the investigation of beam phase variations under dynamic operational conditions, including changes in insertion device gaps and booster ramping cycles. This paper presents the operational principles, implementation architecture, and representative experimental results of the developed detector system.

INTRODUCTION

The Taiwan Photon Source (TPS), located at the National Synchrotron Radiation Research Center, is a third-generation synchrotron light source operating at an electron energy of 3 GeV with a nominal stored beam current of 500 mA [1]. The storage ring is equipped with two superconducting radio-frequency (SRF) cavities, designated SRF2 and SRF3, to support high-current beam operation [2]. The radio-frequency (RF) system operates at a frequency of approximately 499.654 MHz with a harmonic number of 864. The booster ring (BR) is equipped with a single normal-conducting RF cavity, designated as BRF, and operates with a harmonic number of 828.

Synchronization of the RF systems requires precise distribution of a master clock signal. The master clock is located in the 22nd control instrumentation area (CIA) and is distributed to the SRF2 and SRF3 systems located in the 15th and 17th CIAs, respectively, via Libera Sync modules. For the BRF system, a phase-stabilized coaxial cable (PSCC) is employed to deliver the master clock signal with minimal phase drift.

To monitor the phase stability of signals delivered to the RF systems, a phase monitoring system was implemented using the Libera Brilliance+ (LB+) platform [3]. In addition to RF reference monitoring, the system is also capable of tracking the phase of the cavity field in the SRF cavities, as well as the beam phase in both the storage ring and booster ring.

PHASE MONITORING SYSTEM FOR DIAGNOSTICS

To measure the RF phase, two beam position monitoring (BPM) modules and one timing module are installed on the LB+ platform located in the 17th CIA, as illustrated in Fig. 1. The revolution clock and a 3 Hz trigger signal are delivered from the TPS timing system to the timing module. The RF reference signal is provided by the master clock located in the 22nd CIA and transmitted via a PSCC.

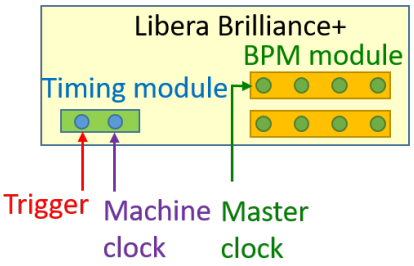

Figure 1: Setup of the beam phase detector, consisting of two beam position monitoring (BPM) modules and one timing module installed on the platform.

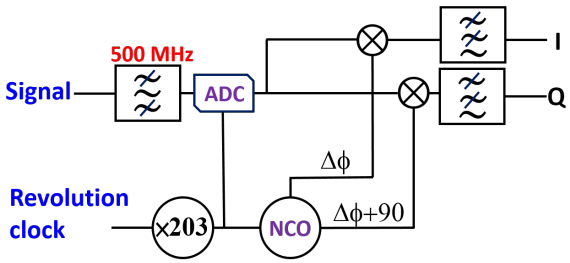

Figure 2: Infrastructure of the beam phase detector. The analog-to-digital converter (ADC) clock is generated by multiplying the revolution clock, while a numerically controlled oscillator (NCO) produces digital signals with a 90-degree phase difference.

Monitor signals—including the RF reference, cavity field signals, and beam signals—are also routed to the BPM modules in the 17th CIA through coaxial cables. As shown in Fig. 2, only the revolution clock is sent to the timing module. Consequently, the analog-to-digital converter (ADC) sampling frequency is derived by multiplying the revolution frequency by a factor of 203, and is therefore not phase-locked to the master clock.

To compensate for this, the RF reference signal from the master clock is directly injected into the first channel of the first BPM module. The in-phase (I) and quadrature (Q) components of the input signals are extracted digitally and the relative phase ϕ_0 with respect to the ADC clock is calculated using:

$$\phi_0 = tain^{-1}(Q/I). \quad (1)$$

* huang.james@nsrrc.org.tw

ISBN: 978-3-95450-262-2 ISSN: 2673-5350 doi: 10.18429/JACoW-IBIC2025-WEPMO29

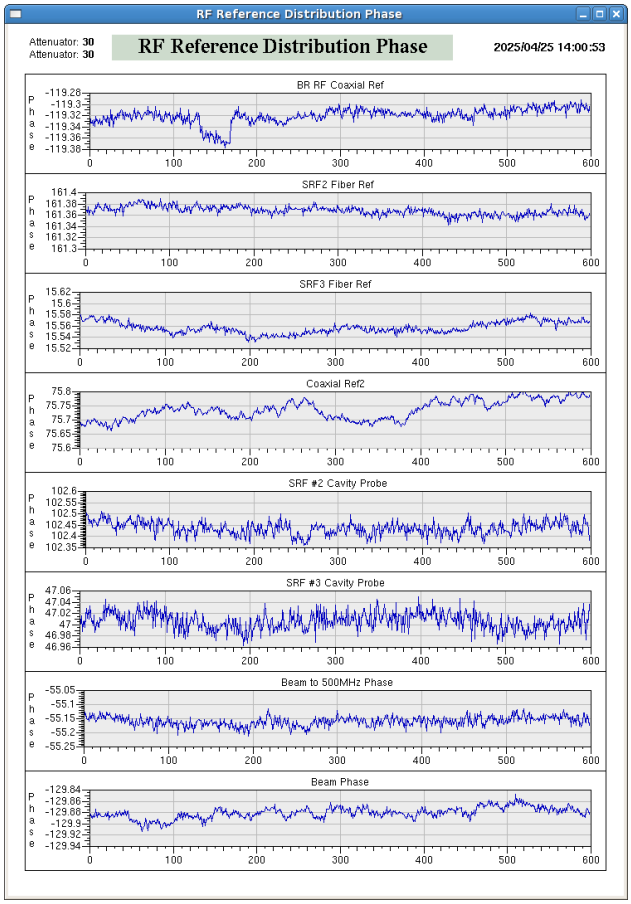

Figure 3: Graphical user interface (GUI) of the phase detector, displaying real-time monitoring of RF phase signals, cavity field phase, and beam phase with 3 Hz sampling rates.

Other measured signals are sent to the BPM module, where their phase relative to the ADC clock is calculated using a similar method. Consequently, the phase relative to the master clock corresponds to the phase with respect to ϕ_0. The BPM electronics provide the in-phase (I) and quadrature (Q) components at a turn-by-turn (TBT) sampling rate via process variables (PVs), allowing the phase information to be retrieved at the same rate. To enable long-term monitoring, the data are downsampled to 3 Hz, displayed in the graphical user interface of the TPS (as shown in Fig. 3), and stored in the archive system.

RADIO FREQUENCY PHASE STABILITY ANALYSIS

Partial RF power is tapped and routed through coaxial cables to a phase detector for phase stability monitoring, prior to transmission to the RF system. As shown in Fig. 4, the short-term variation indicates that the BRF exhibits the largest phase fluctuation, whereas the SRF3 demonstrates the most stable performance. This is attributed to the RF signal path lengths, which are longest in the BRF system and shortest in the SRF3 system. Furthermore, since the RF signal for the BRF system is provided by the PSCC, it must

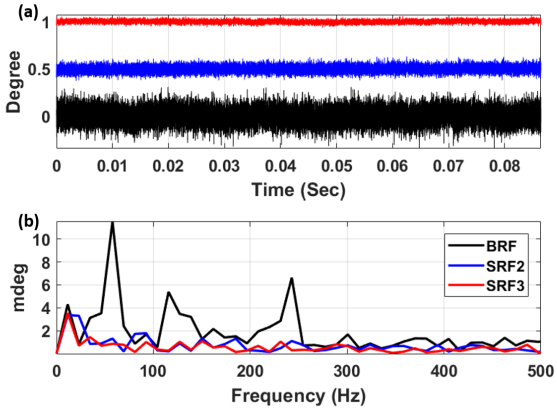

Figure 4: (a) Phase variation of the radio-frequency (RF) signal; (b) frequency spectrum of the RF phase variation.

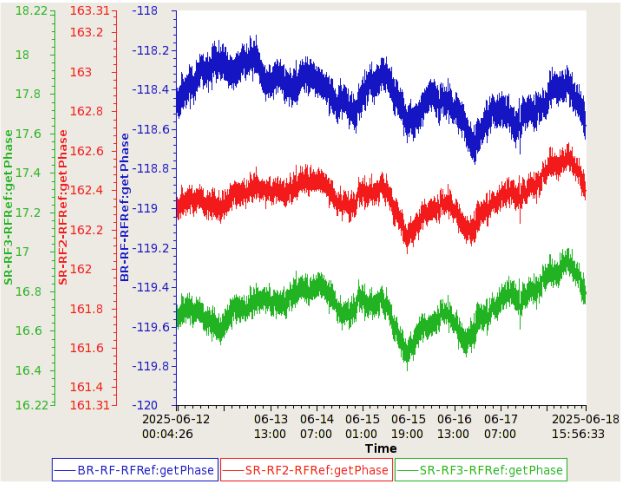

Figure 5: Long-term phase monitoring of the radio-frequency (RF) signals.

be amplified before being delivered to both the BRF system and the phase detector. As a result, the BRF phase spectrum contains frequency components associated with the mains and its harmonics. For long-term monitoring, as depicted in Fig. 5, the standard deviation (STD) of the phase variation remains below 0.1 degrees.

VARIATION OF THE CAVITY FIELD DURING BEAM INJECTION.

During the injection process from 0 mA to 500 mA, as represented by the blue line in Fig. 6, the digital low-level radio frequency (LLRF) system is employed to regulate both the phase and amplitude of the cavity fields. As a result, the phase of the cavities in SRF2 remains nearly constant throughout the injection, as indicated by the red line in Fig. 6. As the beam current stored in the ring increases, a significant discrepancy in forward power between SRF2 and SRF3 emerges, as shown by the magenta line in Fig. 6. To balance the forward power between the RF systems, the station phase of SRF3 is adjusted (black line), which subsequently causes

ISBN: 978-3-95450-262-2 ISSN: 2673-5350 doi: 10.18429/JACoW-IBIC2025-WEPMO29

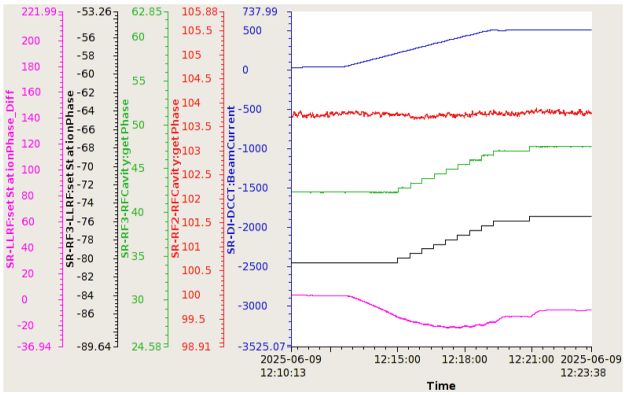

Figure 6: Phase variation of the cavity field during beam injection.

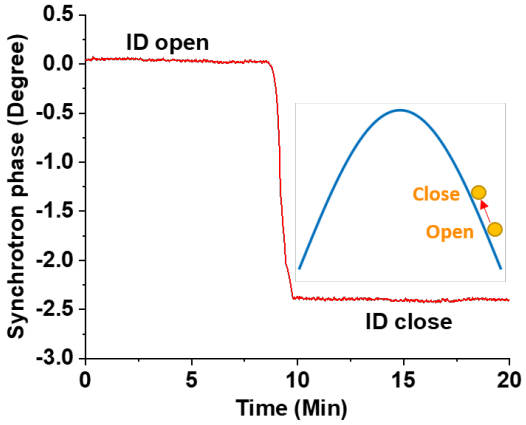

Figure 7: Synchrotron phase shift observed during the closing of the insertion device gaps.

an immediate change in the cavity phase of SRF3 (green line).

IMPACT OF INSERTION DEVICE GAP ON SYNCHROTRON PHASE

The synchrotron phase (ϕ_s) of an electron beam refers to the instantaneous RF electric field phase experienced by an ideal'synchronous particle' as it traverses the RF cavity. There are two SRF cavites that operate with nearly identical gap voltage, so the phase (ϕ_c) of two cavities equals half of the sum in each cavity. When the beam relative to the master (ϕ_b) is determined, the synchrotron phase (ϕ_s) equals ϕ_c - ϕ_b. When the gap of the insertion device is closed, the electron loses more energy during traveling in each circle and the beam phase would decrease to locate at higher RF voltage to gain more RF power as shown in Fig. 7.

SYNCHROTRON PHASE SHIFT DURING BOOSTER RING RAMPING

During the ramping process of the booster ring, the synchrotron phase can be characterized by Ref. [4].

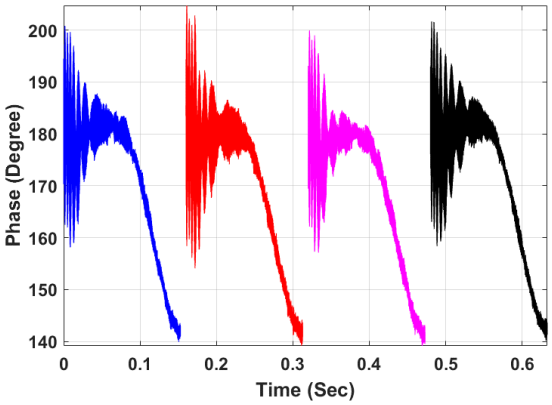

Figure 8: Synchrotron phase variation observed across four injection shots.

$$\sin \phi_s = \frac{88.5E^4\ [\text{GeV}]}{\rho\ [\text{m}]\ V_{\text{RF}}\ [\text{keV}]}. \tag{2}$$

where E is the beam energy, ρ is the bending radius of the dipole magnet, and V_{RF} is the gap voltage of the RF system. In the TPS, ρ is equal to 12.223 m. Generally, during the ramping process, the RF gap voltage does not scale with the fourth power of the beam energy, resulting in observable synchrotron phase shifts, as shown in Fig. 8. At the start of the ramping cycle, three electron bunches from the linac are injected and captured by the RF field with a phase separation of approximately 60 degrees. This causes large phase oscillations to be detected until the three bunches merge into a single bunch. After merging, the remaining phase shift is primarily attributed to the mismatch between the RF gap voltage and the beam energy.

CONCLUSION

A phase detector is set up using BPM electronics to monitor the radio frequency (RF) phase delivered to the RF system, the cavity field phase, and the beam phase in both the storage ring and booster ring, with turn-by-turn (TBT) and 3 Hz sampling rates. The 3 Hz data are also stored in the archive system for subsequent analysis. Regarding the short-term stability of the RF signal delivered to the RF system, the signal to the booster RF system is less stable due to its longer transmission distance and the use of a phase-stabilized coaxial cable instead of an optical fiber with active feedback control. This system can also be employed to monitor the cavity field phase and compute the beam phase during routine operations, including variations in insertion device gaps and beam phase changes during energy ramping in the booster ring.

REFERENCES

[1] C.-C. Kuo *et al.*, "Commissioning of the Taiwan Photon Source", in *Proc. IPAC'15*, Richmond, VA, USA, May 2015, pp. 1314–1318. doi:10.18429/JACoW-IPAC2015-TUXC3

ISBN: 978-3-95450-262-2 ISSN: 2673-5350 doi: 10.18429/JACoW-IBIC2025-WEPMO29

[2] Ch. Wang *et al.*, "System Integration and Beam Commissioning of the 500-MHz RF Systems for Taiwan Photon Source", in *Proc. IPAC'16*, Busan, Korea, May 2016, pp. 2234–2236. doi:10.18429/JACoW-IPAC2016-WEPMB052

[3] E. Buratin *et al.*, "New Measurements Using Libera-Spark Electronics at ESRF: The High Quality Phase-Monitor and the Single-Electron", in *Proc. IBIC'22*, Kraków, Poland, Sep. 2022, pp. 129–132. doi:10.18429/JACoW-IBIC2022-MOP35

[4] J. B. Murphy,"Synchrotron light source data book", *AIP Conf. Proc.*, vol. 249, no. 1, p. 1939, 1992.